RAPID COMMUNICATIONS

PHYSICAL REVIEW A VOLUME 30, NUMBER 5 NOVEMBER 1984

Rapid Communications

The Rapid Communications section is intended for the accelerated publication of important new results. Manuscripts submitted to this section are given priority in handling in the editorial office and in production. A Rapid Communication may be no longer than 3½ printed pages and must be accompanied by an abstract. Page proofs are sent to authors, but, because of the rapid publication schedule, publication is not delayed for receipt of corrections unless requested by the author.

Product states of H_3^+, H_2^+, and O_2^+ electron capture in Cs

J. R. Peterson and Y. K. Bae
Chemical Physics Laboratory, SRI International, Menlo Park, California 94025
(Received 9 July 1984)

A new technique to determine the final states and kinetic energies released in dissociative charge transfer is tested successfully on D_2^+, D_3^+, and O_2^+ in a Cs vapor target. D_3^+ yields both D + D + D and D + D_2 channels, D_2^+ yields D + D from predissociation of $D_2(c^3\Pi_u)$ and radiative dissociation of $a\,^3\Sigma_g^+$, and the $X\,^2\Pi_g^+$ and $a\,^4\Pi_u$ states present in O_2^+ yield a surprisingly simple spectrum that is attributed to near-resonant- and Franck-Condon-type selection rules.

Knowledge of the product states of a charge-transfer reaction is often just as important as that of the magnitude of the reaction cross section or rate. To reach a full understanding of the detailed interactions between ions and neutral species, knowledge of the final states is essential. However, for electron capture these details are generally difficult to obtain experimentally because the charge neutrality of the products inhibits energy analysis, and observation of optical emission is often difficult and not always definitive. We report here on a determination of the final states of dissociative electron-capture reactions between H_3^+, H_2^+, and O_2^+ in Cs that yield atomic products. These experiments have made novel use of translational energy spectroscopy on the negative ions formed in subsequent collisions of the atomic products.

In undertaking this work, we were particularly interested in the final products and energies of electron capture by H_3^+ in Cs. This reaction is expected to proceed generally through near-resonant transitions $H_3^+ + Cs \rightarrow H_3^* + Cs^+$ to excited H_3^* states that are about 4 eV (the ionization energy of Cs) below the initial H_3^+ state. Because H_3 is unbound in the ground electronic state, this H_3^* state must then either dissociate to the products $H + H_2$ or $H + H + H$, or radiate to a lower dissociating state.

Some attention has already been given to H_3^+ and H_2^+ charge transfer in Cs. These reactions have influence on several methods of forming H^- beams for use in the neutral beam heating of magnetic fusion energy plasmas. Meyer and co-workers[1] have measured the total cross sections for H_2^+ and H_3^+ at energies above 40 keV and for D_2^+ above 3 keV, and we[2] have recently measured them at lower energies. Cisneros and co-workers[3,4] have studied angular distributions of negative ions and neutral products of D_2^+ and D_3^+ charge transfer in Cs. Recently, an extensive study of $H_2^+ + Cs$ dissociative charge transfer has been carried out by de Bruijn, Neuteboom, Sidis, and Los,[5] using an elegant position-sensitive coincidence method.

Our method of analyzing dissociative charge-transfer product states is comparatively simple, but effective. It makes use of the fact that a small fraction of the atoms resulting from dissociation of the excited products can capture an electron in a second Cs collision and become negative ions before leaving the charge-transfer oven. For example, we can have $H_2^+ + Cs \rightarrow H + H + Cs^+$, followed by $H + Cs \rightarrow H^- + Cs^+$. By measuring the kinetic energies of the negative ions at 0° lab angle, the same techniques used in photofragment spectroscopy[6-8] can be employed to obtain the c.m. energies released in dissociation, and thus to deduce the internal energies of the charge-transfer product states. The large amplification[8] in the transformation of c.m. to lab energies facilitates the resolution of these states. The energy resolution here is somewhat lower than in photofragment spectroscopy because of collisional effects, but it is still quite high.

The experimental arrangement is shown in Fig. 1, which is labeled for H_3^+ incident beams. A magnetically mass-

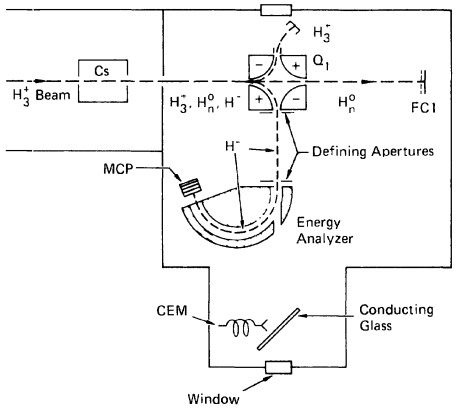

FIG. 1. Schematic of the apparatus.

analyzed H_3^+ beam at energy E_0 undergoes electron capture in an oven containing Cs vapor. The three charge components $(+, 0, -)$ in the emerging beam are separated in an electrostatic quadrupole with a small entrance aperture at 0° along the incident beam axis. H^- ions (with energies near $E_0/3$) are deflected into a small aperture at the entrance to a spherical energy analyzer. The voltages on the deflecting quadrupole and energy analyzer are coordinated to pass the same energies. These ions result from H atoms ejected from the dissociating molecules at 0° and 180° c.m. angles. The ions that emerge from the energy analyzer are accelerated through a potential of several hundred eV to the entrance of a channel plate multiplier, whose output is fed to a count-rate meter. In these first trial measurements the voltages on the deflector and energy analyzer were simply swept slowly by hand, and the count-rate meter output was recorded by an x-y recorder.

$D_3^+ + Cs$. To avoid any possible confusion of D^+ with H_2^+, we used D_2 in the ion source for this first work. The spectrum in Fig. 2 represents the energies of D atoms produced by

$$D_3^+ + Cs \rightarrow Cs^+ + D_3^* \rightarrow D_2 + D \quad (1a)$$

$$\rightarrow D + D + D \ . \quad (1b)$$

The spectrum is asymmetric about $W = 0$ because variations in solid angle, angular scattering, and electron-capture cross sections reduce the detection of the lower lab energy atoms ejected near 180° c.m., compared to those near 0°. We interpret the central peak in Fig. 2 as due to atoms from the D + D + D products (1b), but the bumps on the wings are from $D_2 + D$ (1a). In addition to the asymmetry, the spectrum distorts a straightforward assessment of the relative contributions as a function of W because (a) the laboratory energy scale is nonlinear in W [see Eq. (2) below] and (b) the c.m. solid angle subtended by the detector is strongly dependent on W. It is sharply peaked at $W = 0$, where each atom is traveling at 0° lab angle and is detectable. As W increases the c.m. velocity of the atoms expands the apex angle of the cone in the lab system that includes all c.m. angles, reducing the c.m. solid angle of the detectable ions as $(E - E_0/3)^{-2}$. Figure 3 shows a preliminary deconvolution of the forward-ejected half of the spectrum in Fig. 2, which accounts for this effect. It does not account for the broadening due to scattering or the causes of the amplitude asymmetry discussed above, but it does show that the contributions from the two channels (1a) and (1b) are of comparable magnitudes.

The energy analysis of the spectra depends on the masses and number of the dissociation fragments.

Case A (two fragments, masses m_1 and m_2): In this case the lab energy of m_1 is

$$E_{m_1} = (m_1 + m_2)^{-1}[m_1 E_0 + m_2 W \pm 2(m_1 m_2 E_0 W)^{1/2}] \ , \quad (2)$$

where the W is the total c.m. kinetic energy released. The "amplification" of W in the lab frame occurs through its multiplication by E_0 in the last term.

Case B (separation into D + D + D): In the three-body study case, some model of the dissociating mode must be assumed in order to determine the dynamics. We consider two examples.

(1) The atoms separate at equal c.m. angles, and thus have equal momenta. For equal mass particles, the energies of a fragment at 0° in the lab are given by

$$E_D = \tfrac{1}{3}[E_0 + W \pm 2(E_0 W)^{1/2}] \ . \quad (3)$$

(2) Only two particles leave the center of mass, with opposite momenta: D ← D → D. In this case

$$E_D = E_0/3 + W/2 \pm (2E_0 W/3)^{1/2} \ . \quad (4)$$

Values of W corresponding to the lab energy E_D in Eqs. (2), (3), and (4) are shown in Figs. 2 and 3.

The deconvolution used in Fig. 3 gives a much more accurate picture of the reaction product energies and channel branching than the raw data in Fig. 2, so we will discuss the results shown in Fig. 3. The spectrum can be partitioned

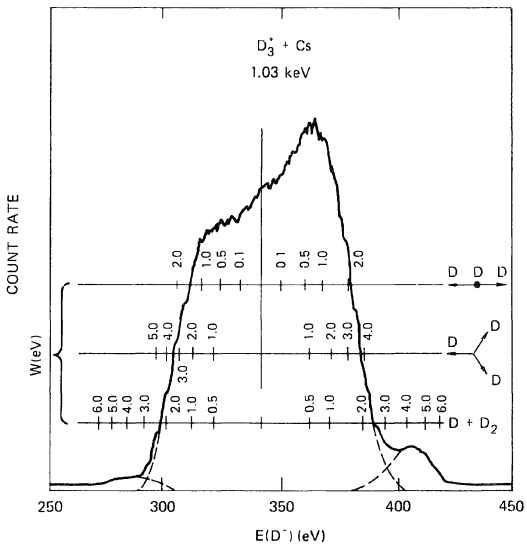

FIG. 2. Laboratory kinetic energies of D atoms produced at 0° (lab) from 1.03-keV $D_3^+ + Cs$. The three insert energy scales represent W for three decay modes (see text).

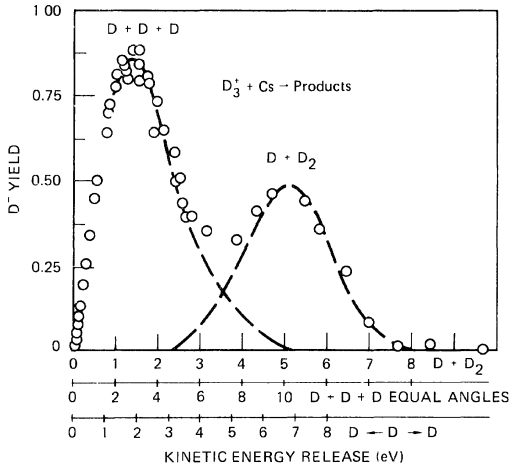

FIG. 3. Deconvolution of the $D_3^+ + Cs$ data in Fig. 2 to account for the W dependence of the c.m. solid angle detected. W scales are appropriate to the indicated decay modes.

into two approximate distributions shown by the dashed lines in Fig. 3, to represent the released energy spectra of the two channels (1a) and (1b).

For D_3^+ ions in the ground vibrational state, the $D_3^+ + Cs$ reaction is exothermic by 0.77 eV for the D+D+D channel and by 5.25 eV for ground-state D_2+D products. The average energy released to the D+D+D channel is about $\overline{W} \simeq 3.5$ eV on the "equal angle" scale, $\overline{W} \simeq 2.4$ eV on the D← D→ D scale, and $\overline{W} \simeq 1.7$ eV on the D+D_2 scale, which represents a limiting model for the unbound D+D+D channel. The actual average is some intermediate value, probably near 2.9 eV. The half-maxima are near 1 and 4.0 eV. From this D+D+D result we can deduce that the D_3^+ ions in the initial beam have internal energies of about 2.2 eV on the average, with half-maxima at about 0.5 and 3.2 eV. The excitation results mostly from the exothermicity of the $D_2^+ + D_2 \rightarrow D_3^+ + D$ reaction that forms the D_3^+ in the ion source, which is 0.8 eV for ground-state reactants. Moreover, the D_2^+ reactants in the ion source are themselves excited by the electron-impact ionization of D_2, with an average energy of about 0.96 eV, estimated from photoelectron spectra.[9]

The D+D_2 channel population peaks at $W \sim 5.1$ eV, with half-maximum values of about 3.8 and 6.3 eV. These values are in excellent agreement with recent $H_3^+ + Cs$ results of de Bruijn *et al.*[10] Considering the 5.8-eV exothermicity of this channel and the initial D_3^+ vibrational excitation deduced from the D+D+D spectrum, the D_2+D spectrum indicates that the D_2 products are internally excited by $\sim 3.6 \pm 1.5$ eV in vibrational-rotational levels.

In considering the relative branching between the D+D_2 and D+D+D channels, one must account for the 3:1 enhanced probability that a D^- will be formed from the latter. With this in mind, the areas under the two peaks in the deconvolution in Fig. 3 indicates that the branching between channels (1a) and (1b) is about 2:1.

$D_2^+ + Cs$. The D^- energy spectrum obtained from $D_2^+ + Cs$ is shown in Fig. 4. The interpretation is the same as that of de Bruijn *et al.*[5] for $H_2^+ + Cs$. The sharp peak between 7 and 8 eV results from predissociation of the $c\,^3\Pi_u$ state to the repulsive $b\,^3\Sigma_u^+$, while the low-energy shoulder is deconvoluted as a broad peak, resulting from radiative decay of $a\,^3\Sigma_g^+$ to $b\,^3\Sigma_u^+$. The deconvoluted spectrum shows that this transition releases an average total kinetic energy of about 2 eV, with a peak probability of about 1.6 eV. Again, the peak at $W = 0$ in Fig. 4 is illusory, owing to the c.m.→ lab solid angle transformation. These preliminary results are in good agreement with the results of de Bruijn *et al.*[5] for 5-keV $H_2^+ + Cs$, but lack the resolution obtained by their technique.

$O_2^+ + Cs$. The O^- spectrum resulting from $O_2^+ + Cs \rightarrow O_2^* \rightarrow O + O$ is shown in Fig. 5. It consists of three peaks centered around ~ 1.2, ~ 3.3, and 7.3 eV. The simplicity of this structure is remarkable, considering the large number of valence states in the O_2 molecule, and as transitions to all three spin manifolds are allowed from the $X\,^2\Pi_g$ and $a\,^4\Pi_u$ states that normally populate O_2^+ beams. It indicates that a fairly high degree of selectivity controls the electron-capture transitions. It seems likely that such a selectivity would favor transitions that satisfy energy-resonance and Franck-Condon criteria, i.e., they terminate on O_2^* potentials about 4 eV (the ionization potential of Cs) below the parent O_2^+ state, and are nearly "vertical."

A tentative analysis of this spectrum, based on these criteria, has been carried out with the use of O_2^+ and O_2 potential energy curves obtained from Krupenie[11] and Saxon and Liu.[12] Only a few states approximately meet the criteria. Figure 6 shows the relevant potentials. The ~2-eV difference betwen the 1.3- and 3.3-eV peaks suggests that these peaks result from states with $O(^3P) + O(^1D)$ and $O(^3P) + O(^3P)$ asymptotic limits, respectively, considering that $O(^1D) - O(^3P) = 1.97$ eV. In Fig. 6, one can see that a single transition to the $1\,^3\Pi_g$ state 3.3 eV above the

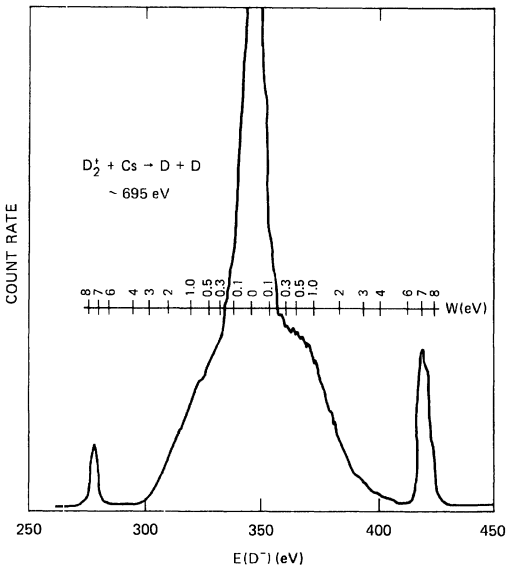

FIG. 4. Laboratory kinetic energies of D atoms at 0° (lab) from 695-eV $D_2^+ + Cs$ reactions.

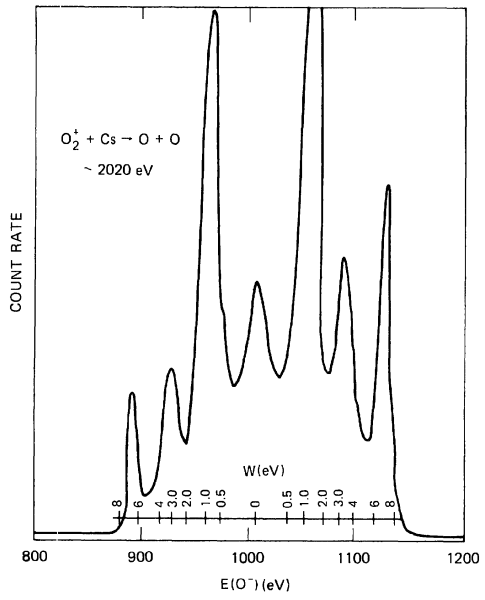

FIG. 5. Laboratory kinetic energies of O atoms from 2020-eV $O_2^+ + Cs$.

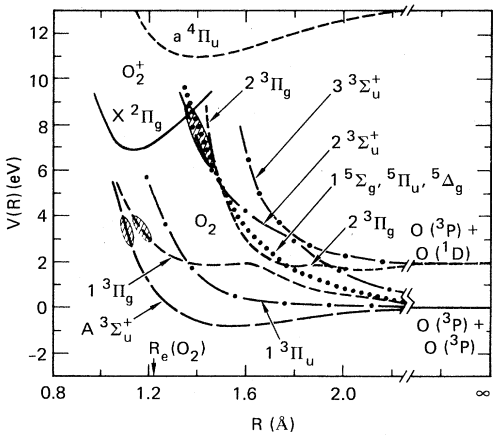

FIG. 6. Potentials pertinent to the $O_2^+ + Cs$ results.

$O(^3P) + O(^3P)$ limit could produce both peaks by branching at the avoided crossing with $2\,^3\Pi_g$ at $R \sim 1.7$ Å. Note that the 3.3-eV level is ~ 4.0 eV below $O_2^+(X)$, and the $1\,^3\Pi_g$ potential is near $R \sim 1.17$ Å at this level, nearly vertically below $R_e(O_2^+X) = 1.12$ Å, in fair agreement with the criteria. Although the 3.3-eV peak can also result from similarly favored transitions to the close-lying $A\,^3\Sigma_u^+$, $A'\,^3\Delta_u$, and $c\,^1\Sigma_u^-$ states (the latter two are not shown in Fig. 6), only $1\,^3\Pi_g$ satisfies both transition criteria for yielding the 1.2-eV peak.

Considering the 7.3-eV peak, we note that 7.3 eV above $O(^3P) + O(^3P)$ is very close to 4 eV below $v = 0$ of $O_2^+(a\,^4\Pi_u)$; hence, this peak can result from a near-resonant electron-capture transition from $O_2^+(a\,^4\Pi_u)$ to a state that dissociates to $O(^3P) + O(^3P)$. Only the nearly degenerate $1\,^5\Sigma_g$, $^5\Pi_u$, $^5\Delta_g$ potentials of Saxon and Liu[11] lie vertically below $O_2^+(a\,^4\Pi_u)$ at 7.3 eV and dissociate only to $O(^3P) + O(^3P)$. The $2\,^3\Sigma_u^+$ potential, also shown in Fig. 6, connects adiabatically to $O(^3P) + O(^3P)$, but an avoided crossing with $3\,^3\Sigma_u^+$ connects to $O(^3P) + O(^1D)$; thus, $2\,^3\Sigma_u^+$ would yield peaks at both 7.3 and 5.3 eV. As we see no evidence of the latter peak, we conclude that the (nearly degenerate) $1\,^5\Sigma_g$, $^5\Pi_u$, $^5\Delta_g$ states produce the 7.3-eV peak.

Because all of the final states of the $O_2^+ + Cs$ electron capture apparently are truly repulsive, these results show in a rather unique and unexpected way the extent that the near-resonance and near–Franck-Condon criteria are both important in selecting the internuclear separations and energies of the final states. We have not considered transitions to intermediate Rydberg states that could predissociate to the final states named above. Such transitions can be ruled out because the results show that the final states are all very close to 4 eV below the initial ion states, and are thus below the level of most Rydberg states leading to that ion limit.

We find that this relatively simple method of analyzing the final states of dissociative charge transfer can be used very effectively for molecules whose atoms have a positive electron affinity. It probably is incapable of the high degree of energy resolution achieved by the elegant technique of de Bruijn *et al.*,[5] but it can examine energy releases down to 0 eV and can be used for triatomic dissociations. It can certainly yield higher-resolution data than were achieved in this brief work.

This work was supported in part by the U.S. Department of Energy through Contract DE-AT03-80ER53091. We have benefited from communications with Dr. D. de Bruijn, Dr. J. Los, Dr. C. Cisneros, Dr. I. Alvarez, Dr. C. F. Barnett, and Dr. A. Russek. The deconvolution program was developed by Dr. Pascale Piquemal. Experimental contributions were also made by Dr. M. J. Coggiola and Dr. P. C. Cosby.

[1]F. W. Meyer, C. S. Anderson, and L. W. Anderson, Phys. Rev. A **15**, 455 (1977); F. W. Meyer and L. W. Anderson, *ibid.* **11**, 589 (1975).

[2]Y. K. Bae, M. J. Coggiola, and J. R. Peterson (unpublished).

[3]C. Cisneros, I. Alvarez, C. F. Barnett, J. A. Ray, and A. Russek, Phys. Rev. A **14**, 88 (1976).

[4]C. Cisneros, I. Alvarez, R. Garcia, C. F. Barnett, J. A. Ray, and A. Russek, Phys. Rev. A **19**, 631 (1979).

[5]D. P. de Bruijn, J. Neuteboom, V. Sidis, and J. Los, Chem. Phys. **85**, 215 (1984).

[6]J. B. Ozenne, D. Pham, and J. Durup, Phys. Lett. **17**, 422 (1972).

[7]N. P. F. B. van Asselt, J. G. Maas, and J. Los, Chem. Phys. Lett. **24**, 55 (1974).

[8]B. A. Huber, T. M. Miller, P. C. Cosby, H. D. Zeman, R. L. Leon, J. T. Moseley, and J. R. Peterson, Rev. Sci. Instrum. **48**, 1306 (1977).

[9]J. Berkowitz and R. Spohr, J. Electron Spectrosc. Relat. Phenom. **2**, 143 (1973).

[10]D. P. de Bruijn *et al.* (private communication).

[11]P. H. Krupenie, J. Phys. Chem. Ref. Data **1**, 423 (1972).

[12]R. P. Saxon and B. Liu, J. Chem. Phys. **67**, 5432 (1977).